A General Method to Determine the Flux of Charged Molecules through Nanopores Applied to ß-Lactamase Inhibitors and OmpF

Supplemental Information

Ishan Ghai,[1] Alessandro Pira,[2] Mariano Andrea Scorciapino,[3] Igor Bodrenko,[2] Lorraine Benier,[1] Matteo Ceccarelli,[2] Mathias Winterhalter,[1] Richard Wagner[1]*

[1]Department of Life Sciences and Chemistry, Jacobs University Bremen, 28719 Bremen, Germany

[2]Department of Physics, University of Cagliari, Cagliari, Italy.

*Corresponding author E-mail: ri.wagner@jacobs-university.de

SUPPORTING INFORMATION

Content:

Materials and Methods

Materials:

Avibactam Sodium. was a gift from AstraZeneca USA, Sulbactam and Tazobactam sodium was obtained from Cayman chemicals USA, Dextran sulfate sodium pharma grade molecular weight 8000 g/mol and Sodium chloride was obtained from Sigma Aldrich Germany, 1,2-diphytanoyl-sn-glycero-3-phosphocholine was procured from Avanti Polar Lipids (Alabaster, AL) and all other chemicals used were procured from AppliChem,

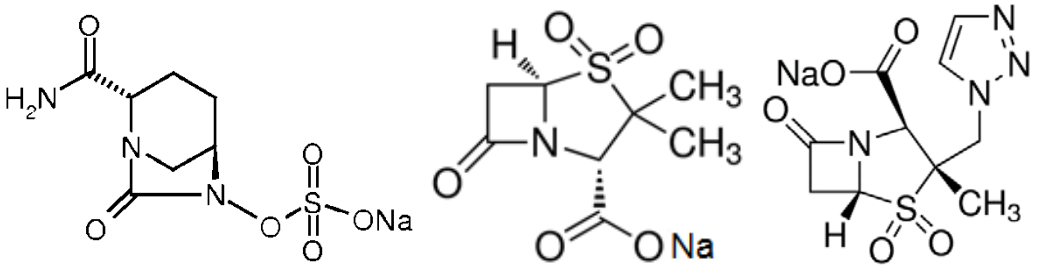

A). Avibactam Na B). Sulbactam Na C). Tazobactam Na

Figure S1. A). Avibactam Sodium, Molecular weight 288 Da. Molecular Formula $C_7H_{10}N_3NaO_6S$. B). Sulbactam Sodium, Molecular weight 255.5 Da. Molecular Formula $C_8H_{10}NNaO_5S$. C). Tazobactam sodium, Molecular weight 322.5 Da. Molecular Formula $C_{10}H_{11}N_4NaO_5S$.

Methods:

Planar Lipid Bilayer and Electrical Recording:

Planar lipid bilayer according to Montal and Mueller were formed as described in detail[1] Briefly, an aperture in a Teflon septum with a diameter of 80−120 μm was prepainted with hexadecane dissolved in n-hexane at 1-3% (v/v) and the chambers were dried for 20-25 min, in-order to remove the solvent. Bilayers were made with 1,2- diphytanoyl-sn-glycerophosphocholine at a concentration of 5 mg/ml in n-pentane. Stock solutions of the outer membrane porin OmpF (0.3-0.5μl 2mg-3mg protein/ml) was added to the cis side for all the measurements. Standard Ag/AgCl or calomel electrodes were used to detect the ionic current. Note that under asymmetric condition we used either homemade salt bridges or commercial calomel electrodes (Metronom). The cis side electrode of the cell was grounded, whereas the trans side electrode was connected to the headstage of an Axopatch 700B amplifier, used for the conductance measurements in the voltage clamp mode. Signals were filtered by an on board low pass Bessel filter at 10 kHz and recorded onto a computer hard drive with a sampling frequency of 50 kHz. Analysis of the current recordings was performed using Clampfit (Axon Instruments). The current voltage relation of the individual experiments was calculated from single averaged currents at the given voltage. All the experiments were repeated three times minimum. Standard solutions contained HEPES 1mM, pH 6, salts and the ß-lactamase-inhibitors at the concentrations given in the (Tables S1). The relative permeability of cations vs inhibitor anions in the bi-ionic case ($P_{Na^+}/P_{inhibitor^-}$) and in the tri-ionic case ($P_{Na^+}/P_{Cl^-}/P_{inhibitor^-}$) were obtained by fitting of the experimental I-V-curves with the Goldman-Hodgkin-Katz current equation[2] but see below for more details.

OmpF conductance under symmetrical low salt bi-ionic conditions

	Inhibitor/salt 30mM (cis/trans)	$\bar{G}_{trimer}$ **(pS) trimer**
OmpF	Avibactam-Na	270 pS ± 60 (n=15)
	Sulbactam-Na	240 pS ± 40 (n=27)
	Tazobactam-Na	240 pS ± 50 (n=36)
	NaCl	270 ± 60 (n=40)
	100 mM NaCl (cis/trans)	960 ±250 (n=10)
OmpF Simulations	NaCl	190± 30 (n=4x200ns)

Table S1: Experimental and calculated conductance of an OmpF-trimer at low ionic strength under bi-ionic conditions, beside the indicted inhibitor or salt concentrations the buffer contained 20 mM HEPES pH 6. Calculated conductance of an OmpF-trimer at corresponding low ionic strength under bi-ionic conditions. V=100 mV and 200 mV respectively for MD modeling.

Electrophysiological permeation assay: Method-Outline

We are interested in obtaining information on the selectivity of the membrane transport of charged antibiotics which are however mostly available in limited quantities and therefore can only be used in trace amounts or lower mM concentrations. To resolve this issue, we apply an experimental setup where a combination of symmetric salt at low concentrations on both sites of the membrane are supplemented with low concentrations of an antibiotic at one site of the membrane (tri-ionic conditions). This setup allows with large pore channels for single channel currents in the range $\ll 100\ pA$ which however can be experimentally resolved.

Assuming single channel recording from a bilayer with an arbitrary channel having the following arbitrary properties:

Permeability: $P_{Na^+} = 4;\ P_{Cl^-} = -1.0;\ P_{AB^-} = 1.0;$

Cation: $z_{Na^+} = 1;\ c_{Na^+cis} = 60\ mM;\ c_{Na\ trans} = 10\ mM$

Anion: $z_{Cl^-} = -1.0;\ c_{Cl^-cis} = 10mM;\ c_{Cl^-trans} = 10mM$

Effector: $z_{AB} = -1.0;\ c_{AB^-cis} = 50mM;\ c_{AB^-trans} = 00mM$

Zero current potential: $V_{rev} = 21.0\ mV\ (experimental\ value)$

Considering that the assumptions of the GHK-theory are valid and the ion fluxes considered to be independent [2] we can calculate the expected current voltage relation for the above membrane channel for any combination of the bi -or tri-ionic concentrations (see Figure S2):

1. $I_{Na^+}(V) = I\left(V, P_{Na^+}, z_{Na^+}, c_{Na^+cis}, c_{Na^+trans}\right),$
2. $I_{CL^-}(V) = I(V, P_{Cl^-}, z_{Cl^-}, c_{Cl^-cis}, c_{Cl^-trans})$
3. $I_{AB^-}(V) = I(V, P_{AB^-}, z_{AB^-}, c_{AB^-cis}, c_{AB^-trans})$
4. $\sum I(V) = I_{Na^+}(V) + I_{Cl^-}(V) + I_{AB^-}(V)$

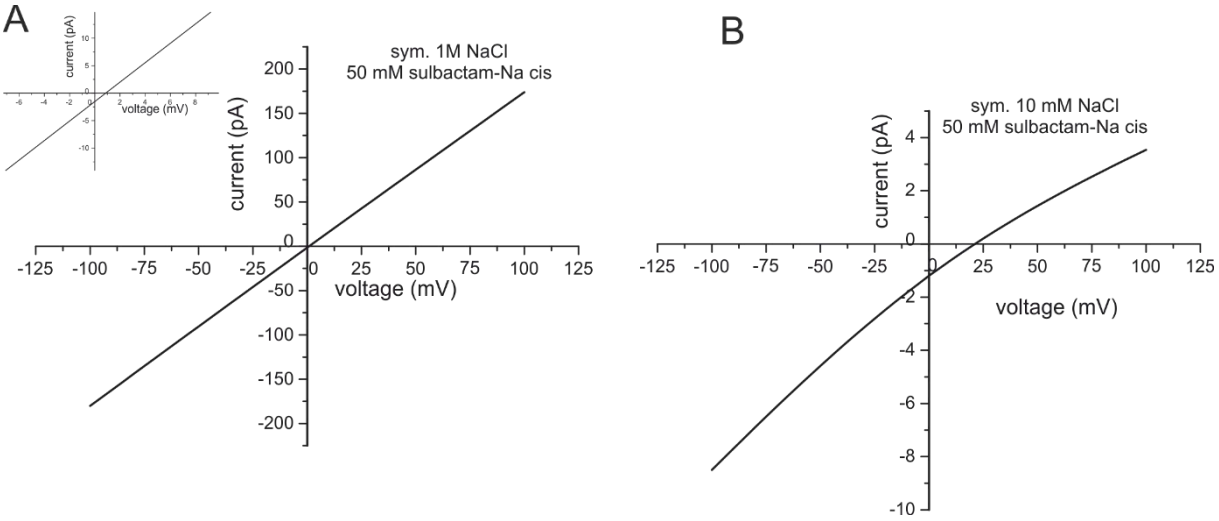

Figure S2: *(**A**) Example for a calculated i-v curve for an arbitrary channel with the above detailed properties with 1M NaCl (cis/trans and cis 50 mM of a charged antibiotic AB with a net charge of -$z_{SB} = -1$. (right)(V_{rev}=0.7mV.) (B) Same as left but with 10 mM NaCl (cis/trans) (V_{rev}=21.3mV)*

For many antibiotic, the solubility is rather limited. As seems in (Figure S2 (A)) 1M NaCl (cis/trans) will mask the change in the reversal potential induced by a 50-mM antibiotic gradient. For an antibiotic concentration of 50 mM (cis) and the conditions above but with 10 mM NaCl (cis/trans) we calculate a $V_{rev} = 21.3\,mV$ a value which can easily be resolved. Straight forward, if under the above described experimental conditions the relative permeability of a channel for the small ions e.g. ($P_{K^+}/\,P_{Cl^-}$) are known and the reversal potential in the additional presence of the antibiotic at a single side has been experimentally

determined it is possible to calculate the relative permeability for the 3 ions ($P_{Na^+} : P_{Cl^-} : P_{AB^-}$) according to the GHK current equation (equation 4) [2].

Sensitivity Limits

Bi-ionic case: In this case V_{rev} is only dependent on the concentration gradient and (P_{cation^+}/P_{anion^-}). However, it is important to note that calomel electrodes are required for the experimental set up since no chloride ions are present in solution.

Considering the case of sulbactam-Na (Figure 1E, Table 2) we observed $V_{rev} = 14{,}3$ (gradient: $\Delta c_{(cis)/trans)}(\frac{80mM}{30mM}) = 2.67$). With the value for $\frac{(P_{Na^+}}{P_{sulbactam^-}} = 4{:}1$ from (Table 2) and an realistic experimental resolution of $\Delta V_{rev} = 1{,}5\ mV$ we end at limiting gradient of Δc =1:1.1.

Tri-ionic Case: In this case classical Ag^+/AgCl electrodes can be used and the reversal potential depends on the concentration of the carrier ions and the concentration of the sulbactam anion at either side of the membrane. Considering again the tri-ionic case of sulbactam-Na (Figure 1B, Table 2) $c_{(cis)} = 50mM$, with 10mM NaCl cis/trans and the experimental $V_{rev} = 21.8$. Taking the permeability values given in (Table 3) but with 1mM NaCl (cis/trans) a concentration of $c_{(cis)} = 250\mu M$ would result in $\Delta V_{rev} = 1{,}5\ mV$ the experimental resolution limit.

Calculation of the Avibactam-anion turnover through OmpF

In order to calculate the turnover number of the avibactam anion through the OmpF pore we used the following data:

(Figure S3A): At a cis/trans 80/30 mM Na-Avibactam gradient: $\frac{P_{avibactam^-}}{P_{Na^+}} = 0.25$ (Table2). Single pore conductance: G_{sp}=90 pS (Avibactam sym. 30mM, cis/trans) (Table 1).

(Figure S3B): At a cis/trans 10/1 µM Na-Avibactam gradient: $\frac{P_{avibactam^-}}{P_{Na^+}} = 0.25$**.** Single pore conductance $\overline{G}_{sp} = 5.6 \cdot 10^{-2}\ pS$. This value was obtained from a Hill plot of the concentration dependence of the OmpF channel conductance for avibactam-Na extrapolated to 10µM avibactam-Na (details not shown).

Using equation (1-4 main text) the relative contributions of the avibactam anion and the Na^+ cation to the total current can be calculated for a single pore and the currents normalized to

the respective $\bar{G}_{sp}$ give the corresponding current voltage relations at the specified ionic conditions (Figure S3A,B).

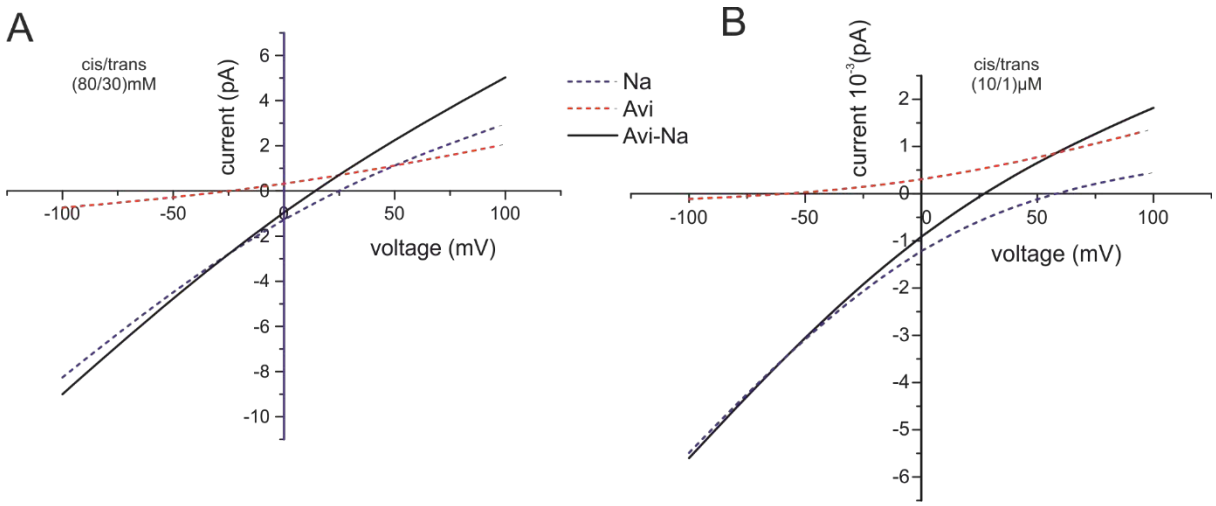

Figure S3: (A) Calculated current voltage relation according to equation (1-4 main text) for a single OmpF channel pore in 80/30 mM Na-Avibactam, using the experimental determined values for $\frac{P_{AB^-}}{P_{Na+}}$ and $\bar{G}_{trimer}$. Dissected current contributions of the avibactam anion (red dots) and the sodium cation (blue dots). (B) Same as (A) but for 10/1 µM avibactam-Na (cis/trans)

For the avibactam anion current at V_m = 0 mV (Figure S3B) we obtain i = 0.001 pA (trimer) the anion flux through a single OmpF pore at the given gradient of Δc=10:1 can be calculated as follows:

$$5. \qquad n = \frac{i \cdot N_A}{F} = \frac{0.001/3 \cdot 10^{-12} \cdot 6.022 \cdot 10^{23}}{964853} = 208\, molecules/s$$

Extended analysis of single channel currents of OmpF in the presence of ß-lactamase-inhibitors

Addition of 10 mM Na-Avibactam (cis) to a bilayer containing a single trimeric OmpF channel did not cause any significant change in the channel gating frequencies and current amplitudes (Fig S4 A and B). OmpF gating with 30 mM (cis/trans) Tazobactam (Figure S7) and Sulbactam (Figure S6) shows, even at 10 kHz time resolution, no significant detectable gating events while the channels remained in the fully open states. Statistical analysis of current traces showed in the case of Avibactam distinct spaced current amplitude patterns of cumulative fast events (see Figure S4E) which presumably are representative for non-

complete time resolved fast gating transitions. Frequency analysis of the electrical current recordings did not give any additional information on the channel gating in the presence of Tazobactam-Na. While OmpF current recordings with 30 mM (cis/trans) Sulbactam showed only rare detectable gating events and all channel pores remained in the fully open states, thus the OmpF channel recordings in the presence of the ß-lactamase inhibitors do not directly provide information on the fluxes of these compounds through the channel. Therefore, from these types of measurements no enlightenment on the permeability of the ß-lactamase anions through OmpF can be obtained.

The three applied ß-lactamase inhibitors showed different effects on the OmpF channel currents.

Since single channel incorporation into the planar bilayer is, particularly at low ionic strength, hardly to achieve we used bilayers containing multiple copies of the trimeric OmpF to analyze the channel properties of single OmpF pores in the presence of the ß-lactamase inhibitors under bi-ionic conditions.

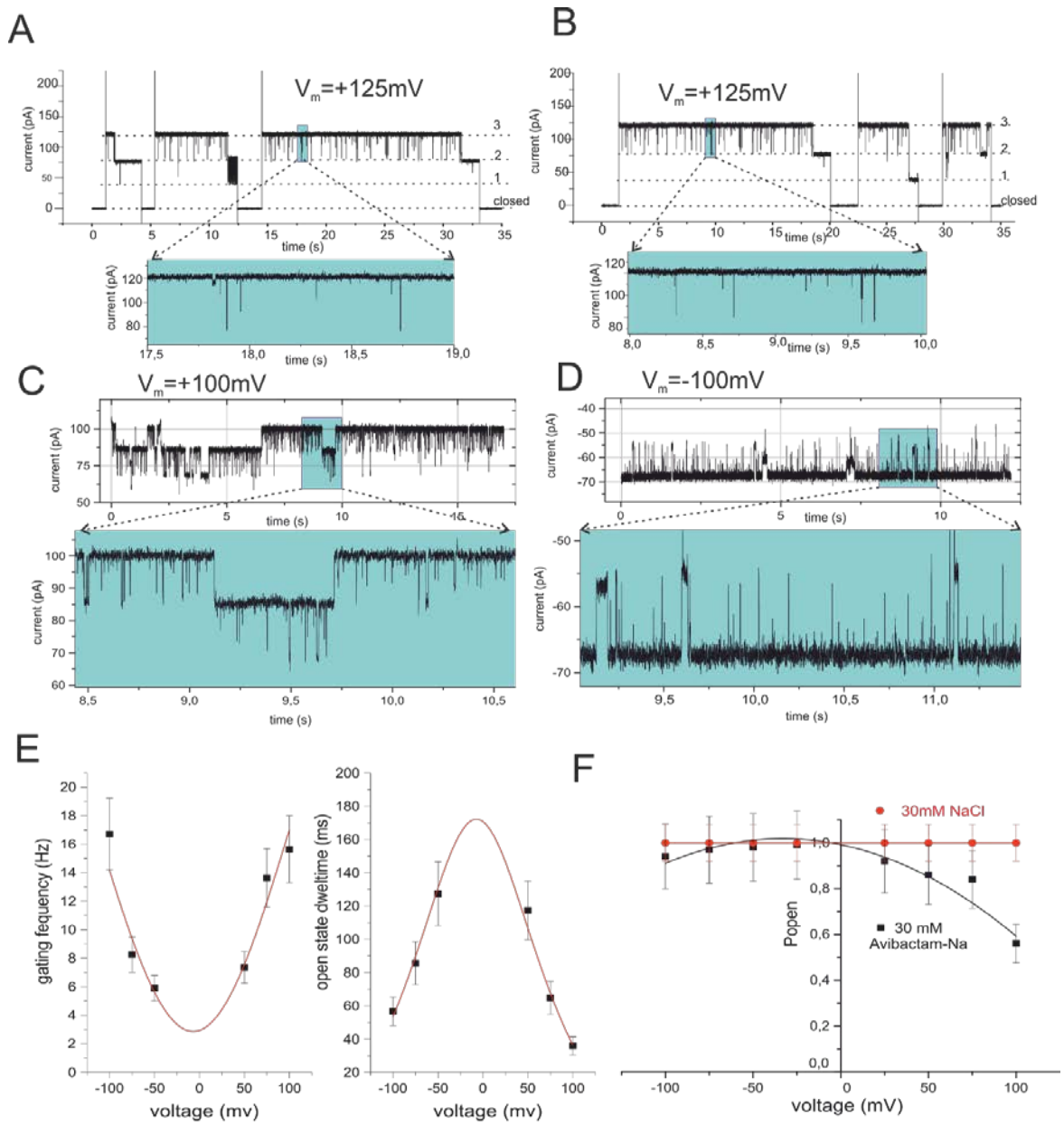

Figure S4: (A, B) Single channel current recording from a bilayer with a single active OmpF channel in 100mM NaCl cis/trans, 20mM HEPES pH 6,0 and applied voltage of V_m=+125mV in absence (A) and presence of 20 mM Na-Avibactam added on cis sides (B). C and D show current recording from a bilayer containing 3 active trimeric OmpF channels in 30mM Na-Avibactam cis/trans, 1mM HEPES pH 6,0 and applied voltage of V_m=+100mV (C) and V_m=-100mV (D). (E) Gating frequency (left) and open state dwell times (right) calculated from current recordings of OmpF containing bilayers in 30mM Na-Avibactam cis/trans, 1mM HEPES pH 6,0, at the indicated V_m (data are mean of 3 independent recordings). (F) Open

probability of a single OmpF channel pore in symmetrically 30/30 mM NaCl (cycles) and 30/30 mM Na-Avibactam, 1mM HEPES pH 6,0..

Avibactam (Figure S5)

Gating of OmpF in the presence Avibactam reveals rare longer closing events in the ms time range mainly at higher V_m and for only parts of the trimeric OmpF pores (Figure S4 E, F). However, the frequency and inter events closing event times occurred random and were neither dependent on the membrane potential nor on the Na-Avibactam concentration. The analysis of the single pore currents (Figure S4 A-F) and the current voltage relation (Figure S5C) revealed that the bilayer contained 4 active trimeric OmpF channels. While the single channel pore conductance in the presence of symmetrical 30 mM Na-Avibactam was $G_{sp} =$ 90 pS (Figure S5E). The effected trimeric OmpF channel remained mainly in the three pores open state even at higher V_m and the channel open probability in the presence of avibactam decreased slightly at higher positive voltages when the Avibactam anion was forced to enter the pore (Figure4F).

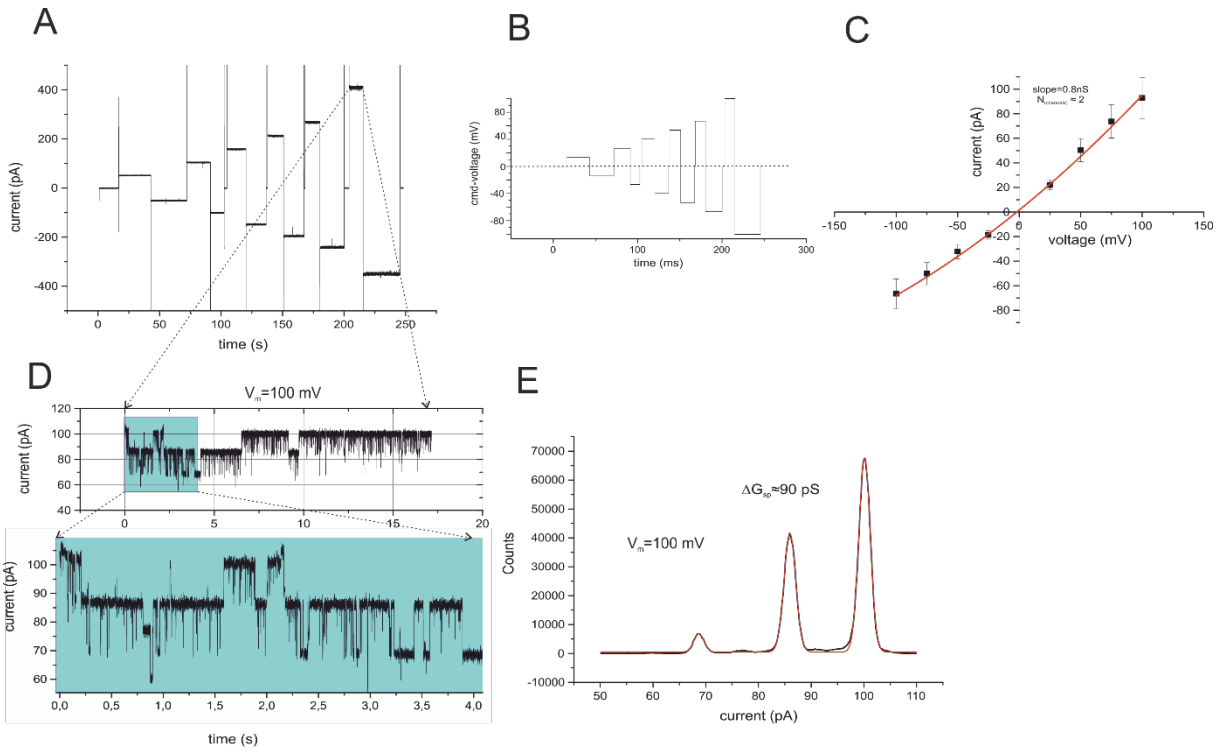

Figure S5: Current recordings from a bilayer containing three active trimeric OmpF channels in the presence of symmetrical 30 mM Na-Avibactam (A): Current recordings of OmpF with symmetrical 30 mM Na-Avibactam. (B) Timeline of the applied voltage steps. (C) Current voltage relation obtained from (A). (D) Expansion of

the current trace at Vm=100 mV (from A). (E) Current amplitude histogram at V_m=100 mV (from A).

Sulbactam (Figure S6)

Current recordings from OmpF containing bilayers in the presence of symmetrical 30mM Na-Sulbactam show almost no detectable gating events and the channels remained in the fully open states (Figure S6 A,D). The analysis of the single pore currents (Figure S6D) and the current voltage relation (Figure S6C) revealed that the bilayer contained 9 active trimeric OmpF channels. While the sing channel pore conductance in the presence of symmetrical 30 mM Na-Avibactam was $G_{sp} = 80$ pS (Figure S5E).

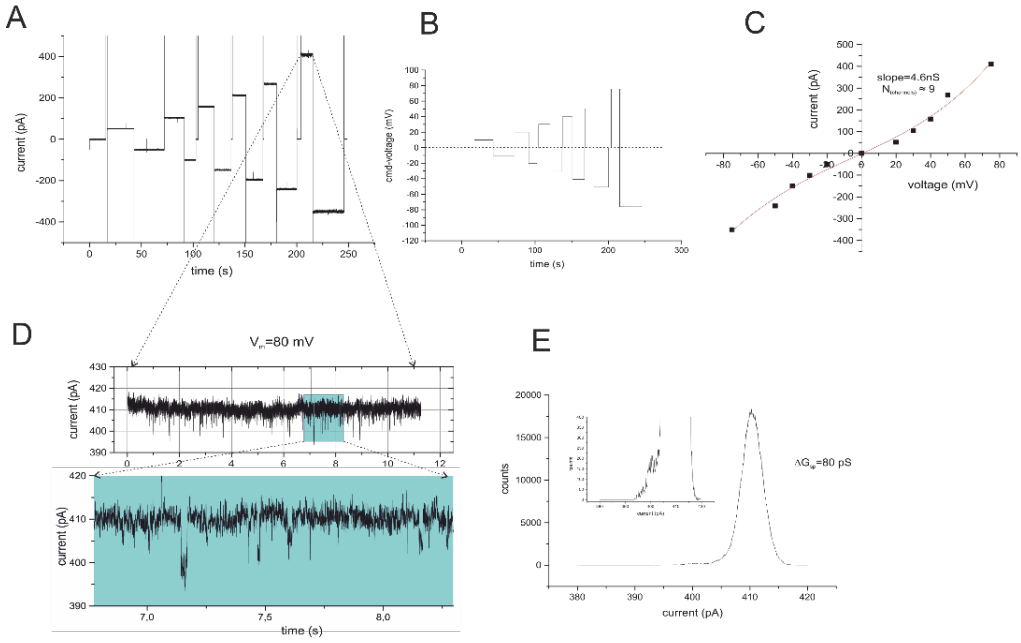

Figure S6: Current recordings from a bilayer containing nine active trimeric OmpF channels in the presence of symmetrical 30 mM Na- Sulbactam

(A): Current recordings of OmpF with symmetrical 30 mM Na-Sulbactam. (B) Timeline of the applied voltage steps. (C) Current voltage relation obtained from (A). (D) Expansion of the current trace at Vm=100 mV (from A). (E) Current amplitude histogram at V_m=100 mV (from A)

Tazobactam (Figure S7)

Current recordings from OmpF containing bilayers in the presence of symmetrical 30mM Na-Tazobactam did not show clearly resolvable 10 kHz gating events of single pores and the channels remain in the fully open states (Figure S7A, C). However statistical histogram analysis of current traces (Figure S7F) shows distinct spacing patterns of cumulative fast current amplitude events which presumably are representative for non-complete resolved fast gating transitions. Frequency analysis unfortunately does not provide any additional information. The analysis of the distinct spacing patterns of cumulative fast current amplitude events (Figure S7F) and the current voltage relation (Figure S7D) revealed that the bilayer contained 5 active trimeric OmpF channels. While the single channel pore conductance in the presence of symmetrical 30 mM Na-Tazobactam was $G_{sp} = 80$ pS (Figure S7F).

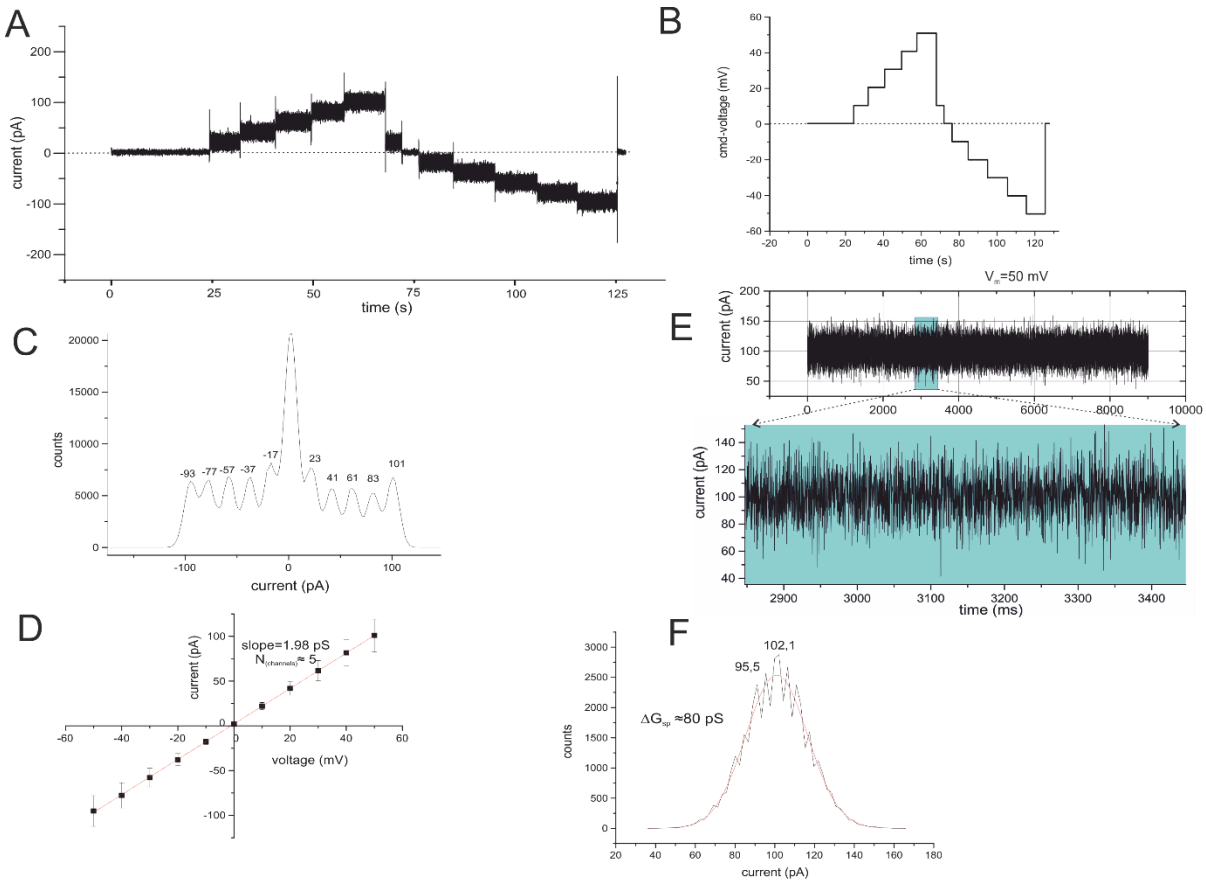

Figure S7: Current recordings from a bilayer containing five active trimeric OmpF channels in the presence of symmetrical 30 mM Na-Tazobactam

(A): Current recordings of OmpF with symmetrical 30 mM Na-Tazobactam. (B) Timeline of the applied voltage steps. (C) All voltage-current amplitude histogram

from (A). (D) Current voltage relation obtained from (A). (E) Expansion of the current trace at V_m=80 mV (from A). (F) Current amplitude histogram at V_m=80 mV (from A).

NaCl (Figure S8)

Current recordings from OmpF containing bilayers in the presence of symmetrical 30mM NaCl show clearly detectable gating events (Figure S10 A, B). The analysis of the single pore currents (Figure S8 A) with the current voltage relation (data not shown) and the current histogram for single pore gating (Figure S8 B) revealed that the bilayer contained 11 active trimeric OmpF channels. While the single channel pore conductance in the presence of symmetrical 30 mM NaCl was $G_{sp} = 88$ pS (Figure S8 B).

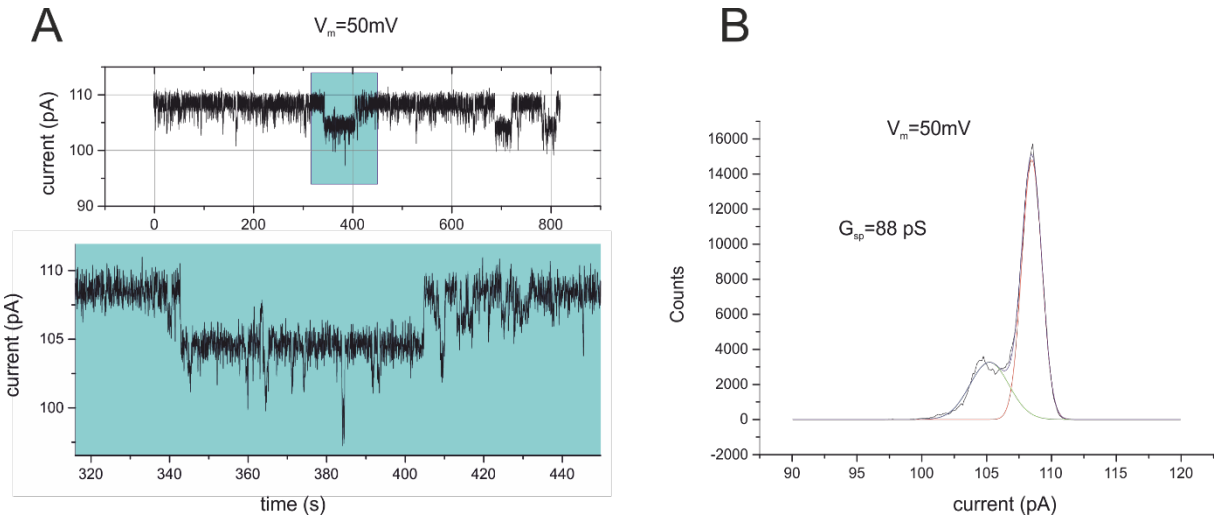

Figure S8: Current recordings from a bilayer containing 11 active trimeric OmpF channels in the presence of symmetrical 30 mM NaCl (A): Current recordings of OmpF with symmetrical 30 mM NaCl. (B) Current amplitude histogram at V_m=50 mV (from A).

Methods: Molecular dynamics simulations

We started from the OmpF structure (PDB ID: 2OMF; 2.4Å resolution) simulated in reference[3]. Briefly, the system was simulated in condition of neutral pH with all amino acid residues in their charged state but for the E296, which was protonated[4]. The OmpF trimer was embedded in a pre-equilibrated POPC (1-palmitoyl-2-oleoyl-sn-glycero-3-phosphocholine) bilayer of 259 lipids. The system was oriented in order to center the protein at the origin of the coordinate system and align the channel along the Z-axis where Z positive values refers to the extracellular vestibule (EV) and Z negative values refers to the periplasmic vestibule (PV).

Thus, the system was equilibrated in vacuum to fill in the gaps. Finally, the system was solvated with ~17000 water molecules and the total number of atoms was ~100k in a box with edges size 11, 11 and 9 nm. A number of potassium and chloride ions were added to have a 0.2 M KCl solution. An excess of K^+ was required to neutralize the negative charges of the trimer (-33 e).

After 1 ps of energy minimization (conjugate gradients), a slow heating from 10 to 300 K was carried out for 1 ns with positional restraints on the Cα protein along three dimensions and on the lipids phosphorus atoms along z only, allowing movement on XY plane. After releasing the constraints, an equilibration stage follows for 4 ns in the NPT ensemble at 1.0 bar and 300 K. Finally, 400 ns MD simulations were performed in the NVT ensemble after the elimination of the protein restraints. Only the last 300 ns were used for the analysis.

Production run in the NVT ensemble was performed through the ACEMD code[5] compiled for GPUs, by rescaling hydrogen mass to 4 au and increasing the time-step up to 4.0 fs. The Langevin thermostat (300 K) was used with 0.1 ps damping time and the particle mesh Ewald (PME) method with 9 Å cut-off for electrostatic interactions. The Amber99sb-ildn force field parameters were used for OmpF, the General Amber Force Field (GAFFlipid) for POPC[6], and the TIP3P model for waters[7]. For Avibactam we used the GAFF approach as described in ref [8]. The three inhibitors were placed above the first monomer in the EV about 20 Å away the constriction region (CR) in the final configuration from the OmpF simulation.

Substrates permeation was investigated using well-tempered meta dynamics simulations with Plumed 2.2 plug-in[9] within the ACEMD software[5]. This method consists in adding Gaussian weight factors that are periodically rescaled providing a convergence parameter to monitor during the meta dynamics simulation[10,11].

A first step of normal metadynamics simulation of inhibitor permeation was performed until the first effective translocation through the protein constriction region (CR) was observed. Then, four configurations were selected, two with the inhibitor located in the extracellular vestibule (EV), and two in the periplasmic vestibule (PV). Correspondingly, four multiple-walkers[12] were set to extend the well-tempered metadynamics reconstruction of the free-energy surface (FES).

The substrates 'position Z' defined as the difference of the z-coordinate between the center of mass (com) of the substrate and that of the porin first monomer (related to Cα) and the 'orientation Φ' of substrate molecular dipole moment related to z component were used as

biased collective variables. Each walker was run for at least 4x450 ns that correspond to a total simulation time of 1.8 μs. During the metadynamics, energy biases were added every 5.0 ps to each collective variable (initial height 1.0 kcal/mol; Δ=5 degree and 0.4 Å for orientation and position, respectively). Well-tempered ΔT was 4800 K (bias factor = 16). Each walker adds its own biases, but it also reads those added by the other walkers, thus accelerating the sampling of the whole space. The one-dimensional free energy surfaces of inhibitors of (Figure. S9) were obtained integrating out the collective variable orientation.

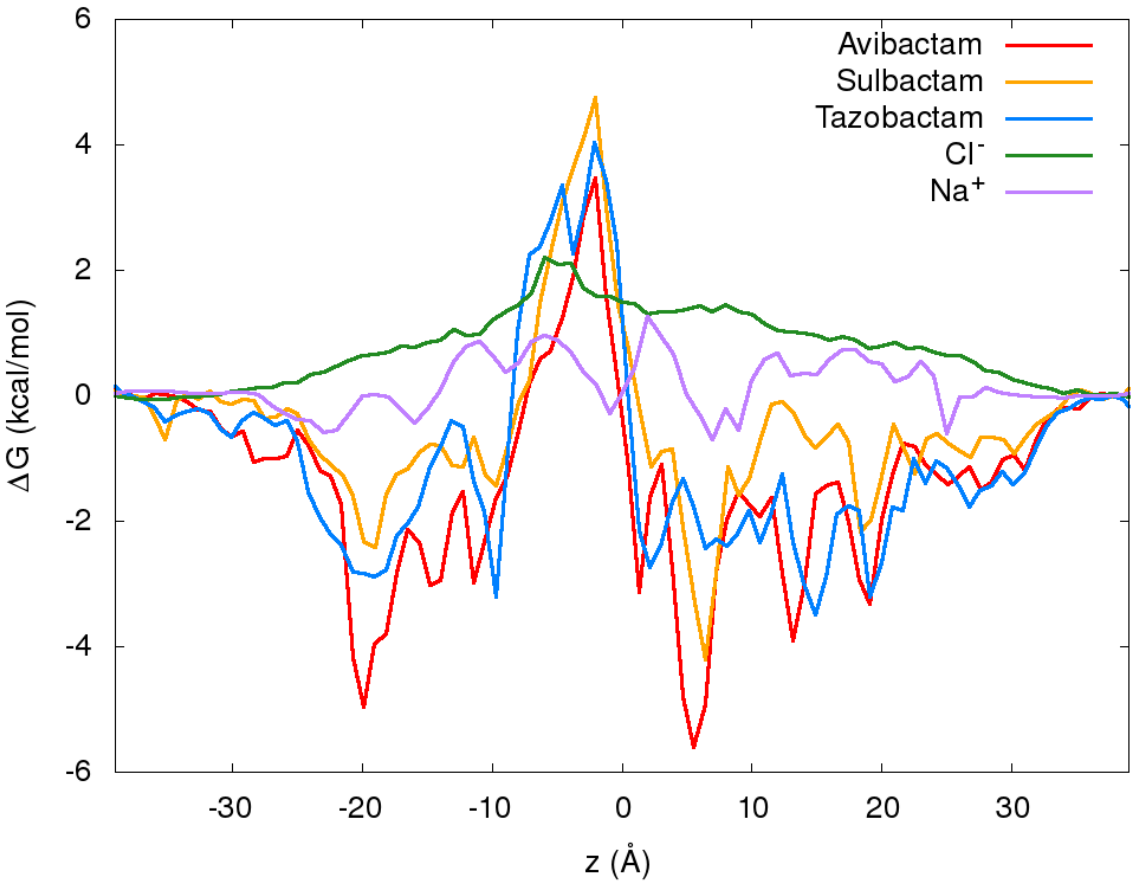

Figure S9: FES reconstructed with metadynamics simulation for the three inhibitors through OmpF, by using two collective variables, namely, molecular dipole orientation and z-coordinate (position along the channel axis). We showed the FES only along the Z coordinate for a comparison with the free energy of ions, calculated with their relative density with respect to the bulk, 200 mM.

Molecular dynamics simulations on the permeation of ions in presence of avibactam

In order to investigate the ion conductance through the trimeric porin, an external electric field was applied using the in-built plugin in ACEMD[5]. A constant force is applied at each atom in the system having a point charge. A representative configuration of the avibactam inhibitor from the minimum found in FES near the constriction region was taken out from

meta dynamics trajectories; 100 steps of energy minimization were performed followed by 10 ns of standard MD simulation equilibration step. Starting from last coordinates obtained by the simulation just described, two different 50 ns simulations were run with external electric field and used as further equilibration step: the first one corresponds to an applied potential of 200 mV and the second one corresponds to an applied potential of -200 mV. Finally, final configurations obtained by both trajectories were used as starting point to run 5 independent simulations for each applied potential. Each simulation was run for 100 ns.

In order to compare the calculated conductance for the systems described above with respect to the case without substrate, an external electric field corresponding to an applied potential of 200 mV and -200 mV were applied to the "empty" system. For each case the first 100 ns MD simulation were used as equilibration step, then 5 independent steps of 100 ns MD simulations were run for both selected applied potential, see (Table S2).

	Without Avibactam			**With Avibactam**		
Empty	**G(pS)**	**K^+/Cl^-**	**Ratio**	**G(pS)**	**K^+/Cl^-**	**Ratio**
1	**830**	**70/36**	**2.0**	**930**	**98/14**	**7.0**
2	**1000**	**96/31**	**3.1**	**970**	**100/22**	**4.6**
3	**860**	**86/24**	**3.4**	**1160**	**107/28**	**3.8**
4	**860**	**78/27**	**2.9**	**870**	**94/19**	**5.0**
5	**830**	**82/27**	**3.0**	**1010**	**101/25**	**4.1**
Average	**880±70**		**2.9**	**990 ±100**		**4.9**
Average K+	**660±70**			**820±60**		
Average Cl-	**210±30**			**170±40**		

Table S2: Conductance and potassium/chloride ratio for the independent standard OmpF MD simulations in presence of 200 mM KCl, without and with avibactam, at 200mV external potential.

Figure. S10: Avibactam (cyan) at positive voltages blocks the chloride path by superimposing to them (green) without affecting the potassium path (violet). The position of avibactam corresponds to the purple minimum of Figure. 2.

References

1. Montal, M. & Mueller, P. Formation of Bimolecular Membranes from Lipid Monolayers and a Study of their ElectricalProperties. Proceedings of the National Academy of Sciences **69,** 3561–3566 (1972).
2. Hille, B. Ionic Channels of Excitable Membranes, Sinauer Ass. Inc., Sunderland, Ma 01375 (2001)
3. Acosta-Gutierrez, S., Scorciapino, M. A., Bodrenko, I. & Ceccarelli, M. Filtering with Electric Field: The Case of E. coli Porins. J Phys Chem Lett **6,** 1807–1812 (2015).
4. Varma, S., Chiu, S.-W. & Jakobsson, E. The Influence of Amino Acid Protonation States on Molecular Dynamics Simulations of the Bacterial Porin OmpF. Biophys J **90,** 112–123 (2006).
5. Harvey, M. J., Giupponi, G. & De Fabritiis, G. ACEMD: Accelerating Biomolecular Dynamics in the Microsecond Time Scale. J Chem Theory Comput **5,** 1632–1639 (2009).
6. Lindorff-Larsen, K. et al. Improved Side-Chain Torsion Potentials for the Amber ff99SB Protein Force Feld. Proteins **78,** 1950–1958 (2010).
7. Jorgensen, W. L., Chandrasekhar, J., Madura, J. D., Impey, R. W. & Klein, M. L. Comparison of Simple PotentialFunctions forSimulating Liquid Water. J Chem Phys **79,** 926 (1983).
8. Malloci, G. et al. A Database of Force-Field Parameters, Dynamics, and Properties of

Antimicrobial Compounds. Molecules **20,** 13997–14021 (2015).
9. Bonomi, M., Barducci, A. & Parrinello, M. Reconstructing the Equilibrium Boltzmann Distribution from Well-Tempered Metadynamics. Journal of Computational Chemistry **30,** 1615–1621 (2009).
10. Barducci, A., Bussi, G. & Parrinello, M. Well-Tempered Metadynamics: A Smoothly Converging and Tunable Free-Energy Method. Phys Rev Lett **100,** 1–4 (2008).
11. Laio, A. & Parrinello, M. Escaping free-energy minima. Proc. Natl. Acad. Sci. U.S.A. **99,** 12562–12566 (2002).
12. Raiteri, P., Laio, A., Gervasio, F. L., Micheletti, C. & Parrinello, M. Efficient Reconstruction of Complex free Energy Landscapes by Multiple Walkers Metadynamics. The Journal of Physical Chemistry. B, Condensed Matter, Materials, Surfaces, Interfaces & Biophysical **110,** 3533–3539 (2006).